

Effective inspiral spin distribution of primordial black hole binariesYASUTAKA KOGA ¹, TOMOHIRO HARADA,² YUICHIRO TADA ^{3,1,4}, SHUICHIRO YOKOYAMA,^{5,6} AND CHUL-MOON YOO¹¹*Division of Particle and Astrophysical Science, Graduate School of Science, Nagoya University, Nagoya 464-8602, Japan*²*Department of Physics, Rikkyo University, Toshima, Tokyo 171-8501, Japan*³*Institute for Advanced Research, Nagoya University, Furocho Chikusaku Nagoya, Aichi 464-8601 Japan*⁴*Theory Center, IPNS, KEK, 1-1 Oho, Tsukuba, Ibaraki 305-0801, Japan*⁵*Kobayashi Maskawa Institute, Nagoya University, Chikusa, Aichi 464-8602, Japan*⁶*Kavli IPMU (WPI), UTIAS, The University of Tokyo, Kashiwa, Chiba 277-8583, Japan*

ABSTRACT

We investigate the probability distribution of the effective inspiral spin, the mass ratio, and the chirp mass of primordial black hole (PBH) binaries, incorporating the effect of the critical phenomena of gravitational collapse. As a leading order estimation, each binary is assumed to be formed from two PBHs that are randomly chosen according to the probability distribution of single PBHs. We find that, although the critical phenomena can lead to large spins on the low-mass tail, the effective inspiral spin of the binary is statistically very small, $\sqrt{\langle\chi_{\text{eff}}^2\rangle} = 8.41 \times 10^{-4}$. We also see that there is almost no anti-correlation between the effective inspiral spin and the mass ratio, which can be inferred from observations.

Keywords: black holes, theory, cosmology

1. INTRODUCTION

The success in the direct observation of gravitational waves from compact binary coalescence have provided us with much information about astrophysics and cosmology. It reveals the abundant existence of massive black holes (see Gravitational Wave Transient Catalog 3 (GWTC-3) (Abbott et al. 2021b) for the latest data up to the end of LIGO–Virgo’s third observing run (O3)), shows us the detail dynamics of kilonova (Metzger 2020) and the properties of high-density nuclear matter (Abbott et al. 2018), constrains theories of modified gravity (Abbott et al. 2019, 2021c),

will be possibly used to measure the Hubble constant of the universe (Abbott et al. 2021a), etc. However, the origin of the source compact objects (black holes in particular) is not fully clear yet, represented by relatively large masses of black holes compared to the known astrophysical models of the black hole formation (e.g., see the implications of the 150 M_{\odot} binary black hole merger (Abbott et al. 2020a) and the compact binary merger in the low-mass gap (Abbott et al. 2020b). Candidate events of subsolar masses, which cannot be stellar black holes, are also reported (Phukon et al. 2021). In addition to the total mass of the binary, the effective inspiral spin $\chi_{\text{eff}} = (a_1 \cos \theta_1 + qa_2 \cos \theta_2)/(1 + q)$ and the mass ratio $q = M_2/M_1$ are other important characteristics of binaries to identify their origins, where M_i , a_i , and θ_i with $i = 1, 2$ are individual masses, individual dimensionless Kerr (spin) parameters, and the angles of individual spins with respect to the orbital angular momentum, respectively. The positive (negative) χ_{eff} indicates the alignment (anti-alignment) of their spins. Callister et al. (2021) and Abbott et al.

koga.yasutaka.k2@f.mail.nagoya-u.ac.jp

harada@rikkyo.ac.jp

tada.yuichiro.y8@f.mail.nagoya-u.ac.jp

shu@kmi.nagoya-u.ac.jp

yoo@gravity.phys.nagoya-u.ac.jp

(2021d) found broad distributions of χ_{eff} and q in the observational data (GWTC-3), allowing the negative χ_{eff} in the posterior particularly for less hierarchical ones $q \sim 1$ (note that there are only two candidate events (GW191109_010717 and GW200225_060421) with significant support, though (Abbott et al. 2021d)). Such a spin anti-alignment is counterintuitive because progenitors' spins are expected to be nearly aligned with their orbital angular momentum if they are isolated. They also remarkably reported a tendency of anti-correlation between the mean value of χ_{eff} and the mass ratio q , that is, the average χ_{eff} has a slightly larger positive value for smaller q , a hierarchical mass configuration. They noted that this tendency is also in an opposite sense to the standard astrophysical models (see Callister et al. (2021) and references therein).

In addition to the astrophysical black hole (ABH), the so-called primordial black hole (PBH) has been also extensively discussed as a candidate of merger black holes (see Bird et al. (2016), Clesse & García-Bellido (2017), and Sasaki et al. (2016) for the first proposals). PBHs are hypothetical black holes formed in the early universe without introducing massive stars contrary to the ordinary ABHs (Zel'dovich & Novikov 1967; Hawking 1971; Carr & Hawking 1974). While many formation mechanisms have been proposed, one main scenario is the collapse of an overdense region of the universe. If primordial density perturbations δ generated by cosmic inflation are large enough and exceed a threshold value δ_{th} , they can gravitationally collapse directly into black holes soon after their horizon reentry (Carr 1975; Nadezhin et al. 1978; Harada et al. 2013). Since the PBH masses are roughly given by the Hubble masses at their formation times, they can be distributed in the very broad range, 10^{-5} – 10^{50} g, including both massive ones and subsolar ones (PBHs with masses smaller than 10^{15} g are considered to have evaporated away by the present epoch due to the Hawking radiation) (Carr 2005).

If we focus on PBHs formed in the radiation dominated era, the spins of PBHs have been thought to be small typically because they originate from the almost spherically symmetric contraction of the Hubble patch. Recently, the spin distribution of PBHs has been extensively studied (Chiba & Yokoyama 2017; Harada et al. 2017; Mirbabayi et al. 2020; He & Suyama 2019; Flores & Kusenko 2021; Chongchitnan & Silk 2021; Eroshenko 2021). In particular, De Luca et al. (2020) and subsequently Harada et al. (2021) carefully investigated it based on the so-called peak theory (Bardeen et al. 1986) of the cosmological perturbation. Harada et al. (2021) found that the root mean square of the initial value of the nondimensional Kerr parameter is given by a form

proportional to $(M/M_H)^{-1/3}$ with a typically small numerical factor of $\mathcal{O}(10^{-3})$, where M and M_H are the PBH mass and the Hubble mass at the formation, respectively. This result implies that, for ordinary formation of PBHs such that $M \sim M_H$, the spin parameter is very small as $\sim 10^{-3}$ in fact. However, according to numerical simulations, the so-called critical phenomena have been reported for the PBH formation on the other hand (Evans & Coleman 1994; Niemeyer & Jedamzik 1998, 1999; Yokoyama 1998; Green & Liddle 1999; Koike et al. 1995; Musco et al. 2005, 2009; Musco & Miller 2013; Escrivà 2020). That is, the resultant PBH mass is not necessarily given by the Hubble mass but in a scaling relation $M \propto M_H(\delta - \delta_{\text{th}})^\kappa$ with the universal power $\kappa \simeq 0.36$. Therefore, the mass can be arbitrarily small as $M \ll M_H$ for $\delta \sim \delta_{\text{th}}$ and rapidly spinning PBHs could be formed in that case. Furthermore, PBHs basically have no correlation with each other because they are separated farther than the Hubble scale at their formation time, which makes the spin anti-alignment more natural for the PBH binaries.

In this paper, based on the above-mentioned observational and theoretical backgrounds, we investigate probability distribution of the effective inspiral spin χ_{eff} , mass ratio q , and chirp mass \mathcal{M} of PBH binaries, taking account of the critical phenomena. In particular, as the mass-spin anti-correlation $\sqrt{\langle a_*^2 \rangle} \propto (M/M_H)^{-1/3}$ is reported, it is interesting to see the correlation between χ_{eff} and q as found in observations. While several scenarios have been proposed for binary formation of PBHs (see, e.g., Nakamura et al. (1997) and Bird et al. (2016)), we simply assume that each binary is formed from two randomly chosen PBHs, considering it as a leading order approximation in any case. Therefore, the probability distribution of the single PBH (Harada et al. 2021) can be straightforwardly extended to the binary system.

This paper is organized as follows. In Sec. 2, we derive the probability distribution of single PBHs incorporating the effect of the critical phenomena of gravitational collapse. For simplicity, we assume an almost monochromatic power spectrum of the density fluctuation that will collapse into a PBH. In Sec. 3, we derive and numerically estimate the probability distribution of PBH binaries formed from two randomly chosen PBHs. The conclusion is given in Sec. 4. We use units in which $c = 1$.

2. DISTRIBUTION OF SINGLE PBHS

Let us discuss the statistics of single PBHs in this section. We focus on the PBH formation via the collapse of overdensities in the radiation-dominated universe. Due to the charge-neutrality of the universe,

PBHs are basically assumed neutral electromagnetically, and hence the no-hair theorem tells us that PBHs are characterized only by their masses M and spin vectors $a^i = a(\sin\theta \cos\phi, \sin\theta \sin\phi, \cos\theta)^T$, where we employ the dimensionless definition $a^i = S^i/GM^2$ with the angular momentum S^i and its norm a is often called *Kerr parameter*. The PBH statistics is accordingly dictated by the probability distribution of their characteristics,

$$P(a, M, \theta, \phi) da dM d\theta d\phi, \quad (1)$$

and the statistical-isotropy assumption restricts its form as

$$P(a, M, \theta, \phi) da dM d\theta d\phi = \frac{1}{4\pi} P(a, M) da dM d\mu d\phi, \quad (2)$$

with $\mu = \cos\theta$, which consistently gives the distribution of the Kerr parameter and mass as

$$P(a, M) = \int P(a, M, \theta, \phi) d\theta d\phi. \quad (3)$$

We below derive this distribution $P(a, M)$.

2.1. Spin distribution

PBHs are supposed to be formed by the collapse of rare highly-overdense regions. According to the *peak theory* (Bardeen et al. 1986), if the density contrast δ follows the Gaussian distribution and characterized by an almost monochromatic power spectrum $\mathcal{P}_\delta(k) \approx \sigma_0^2 k_0 \delta(k - k_0)$ with some scale k_0 as we assume throughout this paper, the spatial profile of such ‘‘high peaks’’ of the Gaussian random field is known to be typically spherically symmetric and given by (Yoo et al. 2018)

$$\delta_{\text{pk}}(r) \simeq \nu \sigma_0 \frac{\sin k_0 r}{k_0 r}, \quad (4)$$

with a (normalized) random Gaussian parameter ν following the distribution $P_G(\nu) = \frac{1}{\sqrt{2\pi}} e^{-\nu^2/2}$. The peak extremum is put at the origin $r = 0$ without loss of generality. The PBH characteristics (mass and spin as well as whether they are really formed or not) are parametrized by this ν parameter. In this subsection, we first review the spin distribution determined by ν , following Harada et al. (2021) (see also Heavens & Peacock (1988) and De Luca et al. (2019)). Note that, although peaks of a Gaussian random field do not necessarily obey a Gaussian distribution, we assume a Gaussian distribution of ν as an approximation. The validity is discussed in Appendix B, and the appropriate normalization factor for the PBH case is given in the next subsection.

Though the typical peak profile is almost spherically symmetric, a slight deviation from an exactly monochromatic spectrum can cause a tidal torque introducing a

spin to a PBH. In the peak theoretical approach, Harada et al. (2021) revealed that the normalized spin parameter h , which is defined in Eq. (A17) of Appendix A, is related to a and ν as

$$h = \frac{a}{C(M, \nu)},$$

$$C(M, \nu) = 3.25 \times 10^{-2} \sqrt{1 - \gamma^2} \sigma_0 \left(\frac{M}{M_H} \right)^{-1/3} \left(\frac{\nu}{10} \right)^{-1}, \quad (5)$$

and follows the universal distribution¹

$$P_h(h) dh = 563h^2 \times \exp \left[-12h + 2.5h^{1.5} + 8 - 3.2(1500 + h^{16})^{1/8} \right] dh, \quad (7)$$

which is a fitting formula found by Heavens & Peacock (1988) (note that it is normalized so that $\int_0^\infty P_h(h) dh = 1$). Here M is the total mass of the collapsing fraction, M_H is the horizon mass at the horizon reentry of the overdense region, and $\gamma := \sigma_1^2/(\sigma_0\sigma_2)$ with $\sigma_j^2 := \int d \ln k k^{2j} \mathcal{P}_\delta(k)$ characterizes the width of the power spectrum of the density contrast ($\gamma = 1$ for an exactly monochromatic spectrum). Throughout this paper, we assume $\gamma = 0.85$. Given M and ν , the PBH spin distribution can be deduced basically from this formula. See Appendix A for the brief introduction of h and $C(M, \nu)$.

One should note that a PBH is not necessarily formed for a given ν and thus the PBH formation condition should be imposed to obtain the spin distribution of PBHs. For an almost monochromatic spectrum (and thus for an almost uniform typical peak profile (4)), it is justified to judge the PBH formation just by whether ν exceeds some threshold value ν_{th} (see, e.g., Germani & Musco (2019)). We basically neglect the spin dependence of ν_{th} but just take account of the fact that $a > 1$ is not allowed for a BH.² That is, we adopt the following

¹ In the recent work (De Luca et al. 2019), another fitting distribution function is given as

$$P_h(h) dh = \exp[-2.37 - 4.12 \ln h - 1.53(\ln h)^2 - 0.13(\ln h)^3] dh. \quad (6)$$

However, since it is singular for $h \rightarrow 0$, we here adopt the original and regular fitting expression (7) given by Heavens & Peacock (1988).

² From the investigations of the critical phenomena in asymptotically flat cases (Baumgarte & Gundlach 2016; Gundlach & Baumgarte 2016; Celestino & Baumgarte 2018), it is implied that the spin dependence of the threshold is weak if the initial matter distribution is nearly spherically symmetric. Since the typical profile of the density perturbation which collapses into a PBH is almost spherically symmetric, the assumption (8) would not greatly affect the resulting distribution of single PBHs.

simplified spin dependence in this paper:

$$\nu_{\text{th}} = \begin{cases} \text{const.} & \text{for } 0 \leq a \leq 1, \\ \infty & \text{otherwise.} \end{cases} \quad (8)$$

Therefore, the distribution of the PBH Kerr parameter a given M and ν is simply obtained by the change of the variable $h \rightarrow a = Ch$ for $0 \leq h \leq 1/C$ as

$$P(a | M, \nu) da = \frac{P_h(a/C(M, \nu))}{C(M, \nu)N_a(M, \nu)} da, \quad (9)$$

with the normalization factor

$$N_a(M, \nu) := \int_0^{1/C(M, \nu)} P_h(h) dh, \quad (10)$$

to ensure $\int_0^1 P(a | M, \nu) da = 1$. The simplified spin dependence (8) does not make a problem practically because the typical PBH spin is quite small as $a \ll 1$ as we will see below.

2.2. Critical behavior

The PBH mass M also depends on ν . It is roughly equivalent to the horizon mass M_H at the horizon reentry of the overdense region, but in detail, it is often assumed to follow the scaling relation,

$$M(\nu) = KM_H(\nu\sigma_0 - \nu_{\text{th}}\sigma_0)^\kappa, \quad (11)$$

through which the PBH mass can be understood as a function of ν . Here $\kappa \simeq 0.36$ is a universal power and K is a weakly profile-dependent coefficient (Evans & Coleman 1994; Escrivà 2020). Since K is of order unity in any case, we here set $K = 1$ for simplicity. Once M is related to ν , the joint probability $P(a, M)$ for a PBH can be calculated as

$$P(a, M) da dM = P(a | M(\nu), \nu) P_\nu(\nu) da d\nu, \quad (12)$$

where

$$P_\nu(\nu) = \sqrt{\frac{2}{\pi}} \frac{e^{-\nu^2/2}}{\text{erfc}(\nu_{\text{th}}/\sqrt{2})}, \quad (13)$$

is the Gaussian distribution of ν for a PBH, i.e., it is defined only for $\nu > \nu_{\text{th}}$ and normalized as $\int_{\nu_{\text{th}}}^\infty P_\nu(\nu) d\nu = 1$ with erfc denoting the complementary error function. For the derivation of Eq. (13), see Appendix B.

The plot of $P(\log_{10} a, \log_{10} M) = P(a, M)(\ln 10)^2 a M$ is shown in Fig. 1 for $\nu_{\text{th}} = 10$ and $\sigma = 0.192$, which correspond to 0.1% fraction of dark matter with $M_H \sim M_\odot$ as will be discussed in the next subsection. The PBH spin and mass are mostly distributed in the range of $10^{-4} \lesssim a \lesssim 10^{-3}$ and $0.1 \lesssim M/M_H \lesssim 0.4$. The

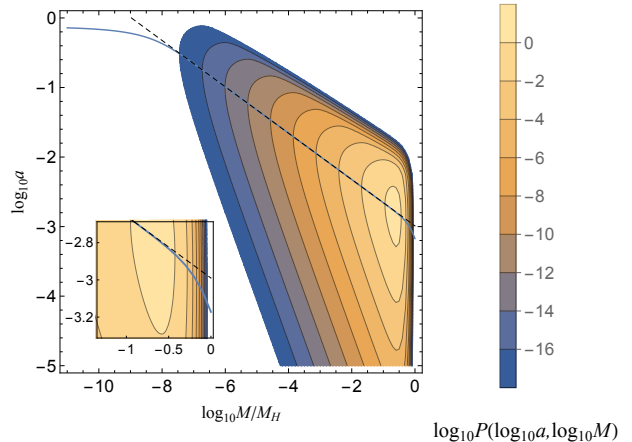


Figure 1. A contour plot of $\log_{10} P(\log_{10} a, \log_{10} M)$ for $\nu_{\text{th}} = 10$ and $\sigma = 0.192$ (see discussions in the next subsection). The solid line shows the expected value $\langle a \rangle$ for each M , while the dashed line is its power-law fitting $\propto (M/M_H)^{-1/3}$.

expected value of a for each M defined by $\langle a(M) \rangle = \int_0^1 a P(a, M) da / \int_0^1 P(a, M) da$ is also plotted. The power law, $\langle a \rangle \propto M^{-1/3}$, can be seen in the range, $10^{-8} \lesssim M/M_H \lesssim 0.3$, as expected from the normalization $C(M, \nu)$ (5) (see Harada et al. (2021)). This anti-correlation between a and M is because, as we can see from Eqs. (A14), (A19), and (A21), the magnitude of the total angular momentum of the collapsing fraction scales as $S_{\text{ref}} \propto (M/M_H)^{5/3}$ and the corresponding Kerr parameter scales as $a \propto A_{\text{ref}} = S_{\text{ref}}/(GM^2) \propto (M/M_H)^{-1/3}$. Also note that this power law is violated for the much smaller mass, $M/M_H \lesssim 10^{-8}$, corresponding to the limit, $\langle a \rangle \rightarrow 1$, because of our assumption that a peak of the density fluctuation with $a > 1$ will not collapse into a PBH. The violation for $M/M_H \gtrsim 0.3$ appears because the factor $\nu(M)^{-1}$ in $C(M, \nu(M))$ is not constant in this range, while it is almost constant, $\nu(M)^{-1} \simeq \nu_{\text{th}}^{-1}$, for $M/M_H \lesssim 0.3$.

2.3. PBH abundance

In order to concretely specify the parameters, let us also review the current PBH abundance. The normalization of ν 's distribution for a PBH (13) implies that a PBH can be formed with the probability $\int_{\nu_{\text{th}}}^\infty P_G(\nu) d\nu = \text{erfc}(\nu_{\text{th}}/\sqrt{2})/2$ at each Hubble patch. Uniformly approximating the PBH mass by the horizon mass for simplicity, the ratio β of the PBH energy density to that of the background radiation at their formation time is hence given by that probability:

$$\beta = \frac{1}{2} \text{erfc} \left(\frac{\nu_{\text{th}}}{\sqrt{2}} \right). \quad (14)$$

After their formation, PBHs behave as non-relativistic matters and their energy density decays as $\propto a^{-3}$ where

\mathbf{a} is the scale factor of the universe. Accordingly, one can calculate the ratio of the current PBH energy density $\rho_{\text{PBH},0}$ to that of the total cold dark matters $\rho_{\text{DM},0}$ and it reads (see, e.g., Tada & Yokoyama (2019))

$$f_{\text{PBH}} = \frac{\rho_{\text{PBH},0}}{\rho_{\text{DM},0}} \sim \left(\frac{\beta}{1.8 \times 10^{-9}} \right) \left(\frac{\Omega_{\text{DM}} h^2}{0.12} \right)^{-1} \left(\frac{g_*}{10.75} \right)^{-1/4} \left(\frac{M}{M_{\odot}} \right)^{-1/2}, \quad (15)$$

where $\Omega_{\text{DM}} h^2 \simeq 0.12$ is the current density parameter of the total cold dark matters (Aghanim et al. 2020), $g_* \simeq 10.75$ is the effective degrees of freedom for energy density of the radiation fluid at the formation time of solar-mass PBHs, and $M_{\odot} \simeq 2 \times 10^{33} \text{ g}$ is the solar mass. Here we approximated the effective degrees of freedom for entropy density by those for energy density, $g_{*s} \approx g_*$, throughout the history and assumed that PBHs were formed at around the time when k_0 reentered the horizon. It has been implied that $f_{\text{PBH}} \sim 0.1\%$ to account for the merger rate of BH binaries inferred LIGO (see, e.g., Ali-Haïmoud et al. (2017) and Vaskonen & Veermäe (2020)). From the formula (15), one sees that this abundance corresponds to $\nu_{\text{th}} \sim 10$ for $M \sim M_{\odot}$. Below, we will employ this value of ν_{th} .

One can also infer the perturbation amplitude σ_0 from the value of ν_{th} . The PBH formation is often judged by using the so-called compaction function $\mathcal{C}(r)$ which is defined by Eq. (4.28) in Shibata & Sasaki (1999) or Eq. (6.33) in Harada et al. (2015) for the constant-mean-curvature slicing. If the maximum $\mathcal{C}_{\text{m}} := \max\{\mathcal{C}(r) | r\}$ exceeds the threshold $\mathcal{C}_{\text{m,th}} \sim 2/5$, which has been suggested by fully non-linear numerical simulations (Shibata & Sasaki 1999; Harada et al. 2015; Musco 2019; Germani & Musco 2019), for some overdense region, that region is supposed to form a PBH. Assuming the peak profile (4), the maximum \mathcal{C}_{m} corresponds to the central value $\delta_{\text{pk}}(r=0)$ by $\mathcal{C}_{\text{m}} \simeq (5/24)\delta_{\text{pk}}(0)$ (see Harada et al. (2021) for details). In order for ν_{th} to correspond to \mathcal{C}_{th} , the perturbation amplitude σ_0 should be given by $\sigma_0 \simeq (24/5)(\mathcal{C}_{\text{m,th}}/\nu_{\text{th}}) \simeq 0.192$.

3. DISTRIBUTION OF PBH BINARIES

As only one PBH forms in one Hubble patch, basically PBHs have no correlation with each other before their formations. They randomly form in space and some of them make binaries by gravitationally catching each other through several proposed scenarios such as free falls of two near PBHs in the early universe (Nakamura et al. 1997) or gravitational captures in galactic halos in the late universe (see, e.g., Bird et al. (2016)). Anyway

two PBHs forming a binary can be assumed to be chosen randomly.

A black hole binary system seen by its merger gravitational waves (GWs) is characterized by the chirp mass \mathcal{M} , the mass ratio q , and the effective inspiral spin χ_{eff} defined by

$$\begin{aligned} \mathcal{M} &= \frac{(M_1 M_2)^{3/5}}{(M_1 + M_2)^{1/5}} \in (0, \infty), \\ q &= \frac{M_2}{M_1} \in (0, 1], \\ \chi_{\text{eff}} &= \frac{a_1 \mu_1 + q a_2 \mu_2}{1 + q} \in [-1, 1], \end{aligned} \quad (16)$$

respectively. Here, the quantities with the subscripts 1 and 2 are those of the primary and secondary PBHs, respectively. The polar angles of spins, θ_1 and θ_2 , are taken so that the axis coincides with the orbital angular momentum, \mathbf{L} . As mentioned, the primary (PBH1) and secondary (PBH2) PBHs are assumed to be chosen randomly according to their probability distribution, Eqs. (1) and (12). Moreover, for simplicity, we assume that the mass and spin angular momenta of PBHs are constant during the formation process of two isolated PBHs to a binary. Thus we can straightforwardly derive the probability distribution of PBH binaries, $P(\mathcal{M}, q, \chi_{\text{eff}}) d\mathcal{M} dq d\chi_{\text{eff}}$ from this single-PBH distribution.

Thanks to the independence of PBH1 and PBH2, one first obtains the joint probability distribution of their intrinsic parameters $\mathbf{w} = (a_1, a_2, M_1, M_2, \mu_1, \mu_2, \phi_1, \phi_2)$ as a direct product of each probability,

$$P(\mathbf{w}) d\mathbf{w} = \frac{2}{(4\pi)^2} \prod_{i=1}^2 P(a_i, M_i) da_i dM_i d\mu_i d\phi_i, \quad (17)$$

where we have normalized the PDF, $P(\mathbf{w})$, so that its integration over $a_i \in [0, 1]$, $0 < M_2 \leq M_1 < \infty$, $\mu_i \in [-1, 1]$, and $\phi_i \in [0, 2\pi)$ becomes unity. Note that the isotropy assumption (2) has been also used. According to the argument on the critical behavior in Sec. 2.2, the distribution of the variables a_i and M_i is read as that of a_i and ν_i by using Eq. (12). Thus, we also have

$$\begin{aligned} P(\mathbf{w}') d\mathbf{w}' &= \frac{1}{8\pi^2} \prod_{i=1}^2 P(a_i | M_i(\nu_i), \nu_i) P_{\nu}(\nu_i) da_i d\nu_i d\mu_i d\phi_i, \end{aligned} \quad (18)$$

for the variables, $\mathbf{w}' = (a_1, a_2, \nu_1, \nu_2, \mu_1, \mu_2, \phi_1, \phi_2)$. Here, ν_i is the peak value of each density fluctuation

that forms each PBH of the binary. Noting the critical behavior (11), the Jacobian reads

$$\begin{aligned} J_{ww'} &= \left| \frac{d\mathbf{w}}{d\mathbf{w}'} \right| \\ &= M_H^2 \kappa^2 \sigma_0^2 (\nu_1 \sigma_0 - \nu_{\text{th}} \sigma_0)^{\kappa-1} (\nu_2 \sigma_0 - \nu_{\text{th}} \sigma_0)^{\kappa-1} \\ &= M_1 M_2 \kappa^2 \sigma_0^2 \left(\frac{M_1}{M_H} \right)^{-1/\kappa} \left(\frac{M_2}{M_H} \right)^{-1/\kappa}, \end{aligned} \quad (19)$$

and the probability in \mathbf{w} is given by

$$\begin{aligned} P(\mathbf{w}) &= J_{ww'}^{-1} P(\mathbf{w}') \\ &= \frac{1}{8\pi^2 J_{ww'}} \prod_{i=1}^2 P(a_i | M_i, \nu(M_i)) P_\nu(\nu(M_i)), \end{aligned} \quad (20)$$

where

$$\nu(M) = \frac{1}{\sigma_0} \left(\frac{M}{M_H} \right)^{1/\kappa} + \nu_{\text{th}}. \quad (21)$$

It can be further translated to the parameter set $\mathbf{z} = (\mathcal{M}, q, \chi_{\text{eff}}, a_1, a_2, \mu_1, \phi_1, \phi_2)$. Recalling the definitions of the effective inspiral spin χ_{eff} , the mass ratio q , and the chirp mass \mathcal{M} (16), the Jacobian from \mathbf{w} to \mathbf{z} can be then computed as

$$\begin{aligned} J_{zw} &= \left| \frac{d\mathbf{z}}{d\mathbf{w}} \right| = \frac{a_2 M_2}{M_1^2 (M_1 + M_2)} \frac{(M_1 M_2)^{3/5}}{(M_1 + M_2)^{1/5}} \\ &= \frac{a_2 q^{11/5}}{(1+q)^{7/5} \mathcal{M}}, \end{aligned} \quad (22)$$

where we used the inverse relation

$$\begin{aligned} M_1(\mathcal{M}, q) &= q^{-3/5} (1+q)^{1/5} \mathcal{M}, \\ M_2(\mathcal{M}, q) &= q^{2/5} (1+q)^{1/5} \mathcal{M}. \end{aligned} \quad (23)$$

The probability in \mathbf{z} is hence found as

$$\begin{aligned} P(\mathbf{z}) &= J_{zw}^{-1} P(\mathbf{w}) \\ &= \frac{1+q}{a_2 q^2 \kappa^2 \sigma_0^2 \mathcal{M}} \left(\frac{(1+q)^{2/5} \mathcal{M}^2}{q^{1/5} M_H^2} \right)^{1/\kappa} \\ &\quad \times \frac{1}{8\pi^2} \prod_{i=1}^2 P(a_i | M_i(\mathcal{M}, q), \nu(M_i(\mathcal{M}, q))) \\ &\quad \times P_\nu(\nu(M_i(\mathcal{M}, q))). \end{aligned} \quad (24)$$

The probability only of \mathcal{M} , q , and χ_{eff} is obtained as the integration over the rest variables a_1 , a_2 , μ_1 , ϕ_1 , and ϕ_2 :

$$P(\mathcal{M}, q, \chi_{\text{eff}}) = \int P(\mathbf{z}) da_1 da_2 d\mu_1 d\phi_1 d\phi_2. \quad (25)$$

Note that the range of μ_1 , originally in $(-1, 1)$, is now restricted by the other variables, χ_{eff} , q , a_1 , and a_2 , as

$$\begin{aligned} \mu_1 &= \frac{(1+q)\chi_{\text{eff}} - qa_2\mu_2}{a_1} \\ &\in \left(\frac{(1+q)\chi_{\text{eff}} - qa_2}{a_1}, \frac{(1+q)\chi_{\text{eff}} + qa_2}{a_1} \right), \end{aligned} \quad (26)$$

because of the range of $\mu_2 \in (-1, 1)$. As a result, we have

$$\mu_1 \in \left(\max \left[-1, \frac{(1+q)\chi_{\text{eff}} - qa_2}{a_1} \right], \min \left[1, \frac{(1+q)\chi_{\text{eff}} + qa_2}{a_1} \right] \right). \quad (27)$$

Finally we obtain the expression

$$\begin{aligned} P(\mathcal{M}, q, \chi_{\text{eff}}) &= \frac{1+q}{2q^2 \kappa^2 \sigma_0^2 \mathcal{M}} \left(\frac{(1+q)^{2/5} \mathcal{M}^2}{q^{1/5} M_H^2} \right)^{1/\kappa} \\ &\quad \times \int_0^1 da_1 \int_0^1 da_2 \Theta(T(a_1, a_2, \chi_{\text{eff}}, q)) T(a_1, a_2, \chi_{\text{eff}}, q) \\ &\quad \times \frac{1}{a_1 a_2} \prod_{i=1}^2 P(a_i | M_i(\mathcal{M}, q), \nu(M_i(\mathcal{M}, q))) \\ &\quad \times P_\nu(\nu(M_i(\mathcal{M}, q))), \end{aligned} \quad (28)$$

where

$$\begin{aligned} T(a_1, a_2, \chi_{\text{eff}}, q) &= \min[a_1, qa_2 + (1+q)\chi_{\text{eff}}] \\ &\quad + \min[a_1, qa_2 - (1+q)\chi_{\text{eff}}]. \end{aligned} \quad (29)$$

By integrating it over one of the three variables, one can further obtain the two-variable probabilities $P(\chi_{\text{eff}}, q)$, $P(\mathcal{M}, \chi_{\text{eff}})$, and $P(\mathcal{M}, q)$. The numerical results are shown in Fig. 2. We take the parameters as $\nu_{\text{th}} = 10$ and $\sigma_0 = 0.192$ which correspond to $f_{\text{PBH}} \sim 0.1\%$ for $M_H \sim M_\odot$ PBHs as discussed in Sec. 2.3.

One can see that the effective spin is distributed in a very narrow region, $|\chi_{\text{eff}}| \lesssim 10^{-3}$. The root mean square is given as $\sqrt{\langle \chi_{\text{eff}}^2 \rangle} = 8.41 \times 10^{-4}$. This would be because, although the effect of the critical phenomena allows each PBH to spin rapidly so that $a \sim 1$ if the mass is very small, the probability of such small mass is very low as can be seen from Fig. 1. The mass ratio is broadly distributed as $0.1 \lesssim q \leq 1$, and the chirp mass has a width $0.1 \lesssim \mathcal{M}/M_H \lesssim 0.3$ due to the critical behavior (11) even though we assume an almost monochromatic power spectrum (i.e., a single value for M_H). In addition, in the plot of $P(\chi_{\text{eff}}, \mathcal{M})$, we can see an anti-correlated behavior between $\sqrt{\langle \chi_{\text{eff}}^2 \rangle}$

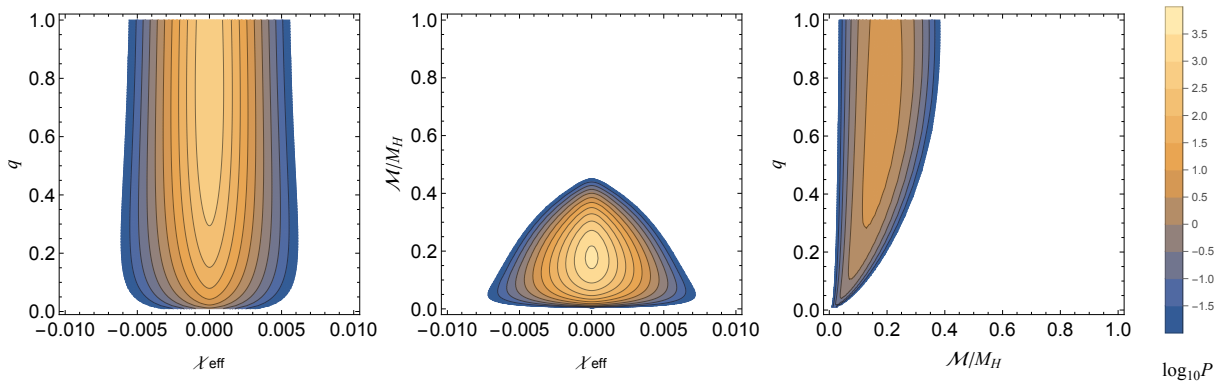


Figure 2. Contour plots of $\log_{10} P(\chi_{\text{eff}}, q)$ (left), $\log_{10} P(\chi_{\text{eff}}, \mathcal{M})$ (middle), and $\log_{10} P(\mathcal{M}, q)$ (right) for $\nu_{\text{th}} = 10$ and $\sigma = 0.192$ which correspond to $f_{\text{PBH}} \sim 0.1\%$ for $M_H \sim M_{\odot}$.

and \mathcal{M} . That is, for smaller \mathcal{M} , the root mean square of the effective spin, $\sqrt{\langle \chi_{\text{eff}}^2 \rangle}(\mathcal{M})$, becomes larger. Actually, by numerical calculation, one can confirm that $\sqrt{\langle \chi_{\text{eff}}^2 \rangle}(\mathcal{M})$ is monotonically decreasing with \mathcal{M} in the range of $3 \times 10^{-4} \lesssim \sqrt{\langle \chi_{\text{eff}}^2 \rangle}(\mathcal{M}) \lesssim 3 \times 10^{-3}$. This is a result expected from the anti-correlation between $\langle a \rangle$ and M for the single PBH distribution. On the other hand, we find that there is almost no correlation between $\sqrt{\langle \chi_{\text{eff}}^2 \rangle}(q)$ and q . In particular, $\sqrt{\langle \chi_{\text{eff}}^2 \rangle}(q)$ cannot be large even for smaller q . This would be because, even if the secondary PBH has a very small mass and therefore has a Kerr parameter of order unity, $a_2 \sim 1$, its contribution to χ_{eff} is suppressed by the very small mass ratio, q , according to the definition (16).

In this paper, as discussed in Sec. 2.3, we have adopted the threshold value of the compaction function, $\mathcal{C}_{\text{m,th}} \simeq 2/5$, which leads to $\sigma_0 \simeq 0.192$ under the assumption $\nu_{\text{th}} = 10$. However, this threshold value would include some uncertainty because the value of $\mathcal{C}_{\text{m,th}}$ slightly depends on the initial profile of the perturbation unlike the averaged one (Escrivà et al. 2020) and the non-zero angular momentum of the collapsing fraction of the universe should make the threshold value higher due to the centrifugal force against the gravitational contraction. We see how this uncertainty affects the resulting distribution in Appendix C by taking different values of σ_0 with the fixed value of $\nu_{\text{th}} = 10$, which we have determined by using Eq. (15). We can see that the modification of σ_0 somehow, but not greatly, changes the widths of the distribution.

4. CONCLUSIONS

In this paper, we formulated the probability distribution of the characteristics (the effective inspiral spin χ_{eff} , the mass ratio q , and the chirp mass \mathcal{M} in particular) of PBH binaries, taking account of the critical phenomena of gravitational collapse. First we have de-

rived the distribution of the spin a and the mass M of single PBHs. It is basically featured by the scaling relation $a \propto (M/M_H)^{-1/3}$ and PBHs with $M \lesssim 10^{-8} M_H$ can have spins of order unity, while the spin is rather suppressed for $M \gtrsim M_H$. Under the assumption that two PBHs of a binary are randomly chosen as a leading order approximation, this single PBH distribution is straightforwardly followed by the binary PBH distribution. The resultant probability in χ_{eff} , q , and \mathcal{M} is shown in Fig. 2.

The first observation is the symmetry under $\chi_{\text{eff}} \leftrightarrow -\chi_{\text{eff}}$, which is a direct consequence of our random-choice assumption. Because of the isotropic distribution of the spin of each PBH, the probability for realizing a binary configuration with the orbital angular momentum \mathbf{L} should be the same as that with $-\mathbf{L}$. This symmetry appears in χ_{eff} , Eq. (16), in terms of the polar angle of each spin, θ_i . That is, the reflection $\mathbf{L} \leftrightarrow -\mathbf{L}$ corresponds to $\theta_i \leftrightarrow \pi - \theta_i$ leading to the symmetry for $\chi_{\text{eff}} \leftrightarrow -\chi_{\text{eff}}$. Actually, Eq. (28) depends on χ_{eff} only through the even function of χ_{eff} , $T(a_1, a_2, \chi_{\text{eff}}, q)$. This symmetry implies that at least a certain fraction of black hole binaries have negative values of χ_{eff} . The negative values of χ_{eff} for black hole binaries with $q \sim 1$ have been indicated by the analyses in Refs. (Callister et al. 2021; Abbott et al. 2021d) although there are only two candidate events (GW191109_010717 and GW200225_060421) with significant support (Abbott et al. 2021d). The PBH binary scenario would have a potential to explain those negative values.

However, the amplitude $|\chi_{\text{eff}}|$ is found to be very small as $|\chi_{\text{eff}}| \lesssim 8.41 \times 10^{-4}$, compared to the observed ones $|\chi_{\text{eff}}| \sim 0.1$. Furthermore, contrary to the anti-correlation between $|\chi_{\text{eff}}|$ and \mathcal{M} as expected from the anti-correlation between a and M in the single PBH distribution, we found almost no correlation between $|\chi_{\text{eff}}|$ and q . This would be because, even though the spin of

the secondary PBH a_2 can be large enough if PBH2 is very light and the mass ratio q is very small, the contribution of a_2 to χ_{eff} is suppressed by the factor q as can be seen its definition (16). Therefore, it would be difficult to realize the observed anti-correlation between χ_{eff} and q in our scenario.

As a further consideration, one may include the clustering effect on the PBH spatial distribution to alter the random-choice assumption. For example, it is known that PBHs are clustered when the source perturbations are non-Gaussian (see, e.g., Sasaki et al. (2018)). Primordial non-Gaussianities may also change the peak statistics and then the spin distribution. Spin evolution through accretion process is also interesting. De Luca et al. (2020) shows the evolution can be significant for massive PBHs $\gtrsim \mathcal{O}(10)M_\odot$. The change of pressure of the background fluid is another possibility to enhance the PBH spins. The pressure p can be reduced from the radiational one $\rho/3$, where ρ is the energy density, dur-

ing, e.g., the quantum chromodynamics (QCD) phase transition or the possible matter-dominated era in the early universe. The reduction of pressure allows a non-spherical collapse and the resultant PBH can have a large spin (Harada et al. 2017). The QCD phase corresponds to $\sim M_\odot$ PBHs and thus it would have a remarkable relation to merger GW events. We leave all these possibilities for future works.

- 1 The authors are grateful to A. Escrivà, S. Hirano,
- 2 T. Kokubu, S. Kuroyanagi, A. Kusenko, and M.
- 3 Sasaki for their fruitful discussions. This work is sup-
- 4 ported by JSPS KAKENHI Grants No. JP21K20367
- 5 (Y.K.), JP19K03876 (T.H.), JP19H01895 (Y.K., C.Y.,
- 6 T.H.), JP20H05853 (Y.K., C.Y., T.H.), JP20H05850
- 7 (C.Y.), JP21K13918 (Y.T.), JP20H01932 (S.Y.) and
- 8 JP20K03968 (S.Y.) from the Japan Society for the Pro-
- 9 motion of Science.

APPENDIX

A. DIMENSIONLESS SPIN PARAMETER h

We have quoted the result for the spin distribution of a single PBH obtained in Harada et al. (2021). In this section, we briefly introduce the relevant quantities for the derivation, especially, the dimensionless spin parameter h . The parameter h was first introduced by Heavens & Peacock (1988) and applied to derivation of PBH spin distribution by De Luca et al. (2019).

Let us consider the 3 + 1 decomposition of the spacetime,

$$ds^2 = -\alpha^2(\eta, \mathbf{x}) d\eta^2 + \mathbf{a}^2(\eta)\gamma_{ij}(dx^i + \beta^i(\eta, \mathbf{x}) d\eta)(dx^j + \beta^j(\eta, \mathbf{x}) d\eta), \quad (\text{A1})$$

with a background flat FLRW metric,

$$ds^2 = \mathbf{a}^2(\eta)(-d\eta^2 + dx^2 + dy^2 + dz^2). \quad (\text{A2})$$

$\mathbf{a}(\eta)$, $\alpha(\eta, \mathbf{x})$, and $\beta^i(\eta, \mathbf{x})$ denote the global scale factor, the lapse function, and the shift vector, respectively. We assume the matter field to be a single perfect fluid,

$$T^{ab} = \rho u^a u^b + p(g^{ab} + u^a u^b). \quad (\text{A3})$$

On the background spacetime, there are rotational Killing vectors $\phi_i^a = \epsilon_{ijk}(x - x_{\text{pk}})^j \delta^{kl}(\partial/\partial x^l)^a$ ($i = 1, 2, 3$) tangent to a spacelike hypersurface $\eta = \text{const.}$ For a region Σ on the spacelike hypersurface, the conserved angular momentum $S_i(\Sigma)$ of the matter con-

tained in Σ can be defined as

$$\begin{aligned} S_i(\Sigma) &:= \frac{1}{16\pi G} \int_{\partial\Sigma} \epsilon_{abcd} \nabla^c(\phi_i)^d \\ &= -\frac{1}{8\pi G} \int_{\Sigma} R^{ab} n_a(\phi_i)_b d\Sigma \\ &= -\int_{\Sigma} T^{ab} n_a(\phi_i)_b d\Sigma, \end{aligned} \quad (\text{A4})$$

where the Einstein equation is used in the last equality. For primordial black hole formation, we suppose Σ to be a region that will collapse into a black hole, and the black hole mass and angular momentum are estimated as those of matter in Σ . Here we assume that the region Σ is given by

$$\Sigma = \{\mathbf{x} \mid \delta(\mathbf{x}) > f\delta_{\text{pk}}\}, \quad (\text{A5})$$

with some positive constant f less than unity.

Around the peak, the density contrast, which we assume to be a Gaussian random field, is expanded as

$$\delta \simeq \delta_{\text{pk}} + \frac{1}{2} \zeta_{ij} (x - x_{\text{pk}})^i (x - x_{\text{pk}})^j, \quad (\text{A6})$$

where

$$\zeta_{ij} := \left. \frac{\partial^2 \delta}{\partial x^i \partial x^j} \right|_{\mathbf{x}=\mathbf{x}_{\text{pk}}}. \quad (\text{A7})$$

Taking x , y , and z axes as the principal directions of ζ_{ij} , we have

$$\delta \simeq \delta_{\text{pk}} - \frac{1}{2} \sigma_2 \sum_{i=1}^3 \lambda_i ((x - x_{\text{pk}})^i)^2, \quad (\text{A8})$$

where σ_j is defined below Eq. (7) and $\lambda_1 \leq \lambda_2 \leq \lambda_3$ are the eigenvalues of $-\zeta_{ij}/\sigma_2$. As a result, Σ is given as an ellipsoid with the three axes,

$$a_i^2 = 2 \frac{\sigma_0}{\sigma_2} \frac{1-f}{\lambda_i} \nu. \quad (\text{A9})$$

Expanding the fluid 3-velocity $v^i := u^i/u^0$ as

$$v^i - v_{\text{pk}}^i \simeq v^i_j (x - x_{\text{pk}})^j, \quad (\text{A10})$$

we obtain

$$\begin{aligned} S_i(\Sigma) &\simeq (1+w) \mathbf{a}^4 \rho_b \epsilon_{ijk} v^k_l \int_{\Sigma} (x - x_{\text{pk}})^j (x - x_{\text{pk}})^l d^3x \\ &= (1+w) \mathbf{a}^4 \rho_b \epsilon_{ijk} v^k_l J^{jl}, \end{aligned} \quad (\text{A11})$$

where $w = p/\rho$ and

$$\begin{aligned} v^k_l &:= \left. \frac{\partial v^k}{\partial x^l} \right|_{\mathbf{x}=\mathbf{x}_{\text{pk}}}, \\ J^{jl} &:= \int_{\Sigma} (x - x_{\text{pk}})^j (x - x_{\text{pk}})^l d^3x \\ &= \frac{4\pi}{15} a_1 a_2 a_3 \text{diag}(a_1^2, a_2^2, a_3^2). \end{aligned} \quad (\text{A12})$$

For PBH formation, we focus on a growing mode of the perturbation. The time dependence of the perturbation is investigated in Harada et al. (2021). According to it, the average of the spin magnitude is decomposed as

$$\sqrt{\langle S_i S^i \rangle} = S_{\text{ref}} \sqrt{\langle s_e^i s_{ei} \rangle}, \quad (\text{A13})$$

where

$$\begin{aligned} S_{\text{ref}}(\eta) &= (1+w) \mathbf{a}^4 \rho_b g(\eta) (1-f)^{5/2} R_*^5, \\ \vec{s}_e &= \frac{16\sqrt{2}\pi}{135\sqrt{3}} \left(\frac{\nu}{\gamma} \right)^{5/2} \frac{1}{\sqrt{\Lambda}} (-\alpha_1 \tilde{v}_{23}, \alpha_2 \tilde{v}_{13}, -\alpha_3 \tilde{v}_{12}), \\ \alpha_1 &= \frac{1}{\lambda_3} - \frac{1}{\lambda_2}, \quad \alpha_2 = \frac{1}{\lambda_3} - \frac{1}{\lambda_1}, \quad \alpha_3 = \frac{1}{\lambda_2} - \frac{1}{\lambda_1}, \\ \Lambda &:= \lambda_1 \lambda_2 \lambda_3, \quad R_* := \sqrt{3} \frac{\sigma_1}{\sigma_2}. \end{aligned} \quad (\text{A14})$$

The function $g(\eta)$ defined by

$$\langle (v^k_l(\eta))^2 \rangle = g^2(\eta) \langle (\tilde{v}^k_l)^2 \rangle, \quad (\text{A15})$$

represents the time evolution of the velocity field for every k, l , where the time-independent variable \tilde{v}^k_l is defined by

$$\tilde{v}^i_j := -\frac{1}{\sigma_0} \int \frac{d^3k}{(2\pi)^3} \frac{k^i k_j}{k^2} \delta_{\mathbf{k}} e^{i\mathbf{k}\cdot\mathbf{z}}, \quad (\text{A16})$$

For large ν limit, the dimensionless spin parameter h is defined by

$$s_e := \sqrt{\vec{s}_e \cdot \vec{s}_e} = \frac{2^{9/2}\pi}{5\gamma^6\nu} \sqrt{1-\gamma^2} h. \quad (\text{A17})$$

h is useful to investigate the probability distribution of the spin. Heavens & Peacock (1988) numerically derived the probability distribution as

$$\begin{aligned} P_h(h) dh &= 563h^2 \\ &\times \exp \left[-12h + 2.5h^{1.5} + 8 - 3.2(1500 + h^{16})^{1/8} \right] dh. \end{aligned} \quad (\text{A18})$$

Recently, De Luca et al. (2019) gave another fitting formula which agrees with the above one very well. In this paper we adopt the former one because of the regular behavior in the limit $h \rightarrow 0$.

The total angular momentum $S_i(\Sigma)$ will become that of the resulting PBH after the formation. The region Σ , which will collapse into a PBH, would be specified when the contraction of matter is decoupled from the expansion of the universe. This is called turn around. We denote the time of turn around as η_{ta} . Defining the dimensionless reference spin value at turn around as

$$A_{\text{ref}}(\eta_{\text{ta}}) = \frac{S_{\text{ref}}(\eta_{\text{ta}})}{GM_{\text{ta}}^2}, \quad (\text{A19})$$

where M_{ta} is the mass inside Σ at the turn around, we can estimate the initial dimensionless Kerr parameter a of the resulting PBH. For the radiation domination, Harada et al. (2021) found, in Eq. (22) of it, the simple expression of $A_{\text{ref}}(\eta_{\text{ta}})$ as

$$A_{\text{ref}}(\eta_{\text{ta}}) \simeq \frac{1}{24\sqrt{3}\pi} x_{\text{ta}}^2 (1-f)^{-1/2} |T_{v\text{CN}}(k_0, \eta_{\text{ta}})| \sigma_H, \quad (\text{A20})$$

where $x_{\text{ta}} = k_0 \eta_{\text{ta}}$, $T_{v\text{CN}}(k_0, \eta)$ is the transfer function of the mode of the velocity field with wavelength k_0 in the conformal Newtonian gauge, and σ_H denotes σ_0 when the initial time of the evolution of the cosmological perturbation is set to the horizon entry. For radiation domination, the factors were numerically estimated as $x_{\text{ta}} \simeq 2.14$ and $T_{v\text{CN}}(k_0, \eta_{\text{ta}}) \simeq 0.622$ in Sec. 3.3 of Harada et al. (2021). Using the relation between M_{ta} and f derived in Harada et al. (2021),

$$M_{\text{ta}} \simeq \frac{\sqrt{6}}{x_{\text{ta}}} (1-f)^{3/2} M_H, \quad (\text{A21})$$

and identifying M_{ta} with M and σ_H with σ_0 , we have

$$A_{\text{ref}}(\eta_{\text{ta}}) \simeq 2.28 \times 10^{-2} \sigma_0 \left(\frac{M}{M_H} \right)^{-1/3}. \quad (\text{A22})$$

Then, we obtain the Kerr parameter of a PBH by putting $a = \sqrt{S_i S^i}/GM^2 = A_{\text{ref}} s_e = Ch$ in terms of

h with a coefficient C , where

$$\begin{aligned} C &= \frac{2^{9/2}\pi}{5\gamma^6\nu} \sqrt{1-\gamma^2} A_{\text{ref}}(\eta_{\text{ta}}) \\ &= 3.25 \times 10^{-2} \sqrt{1-\gamma^2} \sigma_0 \left(\frac{M}{M_H}\right)^{-1/3} \left(\frac{\nu}{10}\right)^{-1}. \end{aligned} \quad (\text{A23})$$

We have set $\gamma^6 \simeq 1$ in the last equality.

B. CORRECTION DUE TO PEAK FINDING CONDITION

We regard the density contrast δ as a Gaussian random field. This implies that its scaling δ/σ_0 is also a Gaussian random field. However, if we focus on its peaks, the probability distribution of the peak values, $\nu = \delta_{\text{pk}}/\sigma_0$, are not given by a Gaussian function because it is corrected by *the peak-finding condition*.

According to [Bardeen et al. \(1986\)](#), the number density of the peaks with the value in $(\nu, \nu + d\nu)$ is given by

$$\begin{aligned} \mathcal{N}_{\text{pk}}(\nu) d\nu &= \frac{1}{(2\pi)^2} \left(\frac{\sigma_2}{\sqrt{3}\sigma_1}\right)^3 e^{-\nu^2/2} \\ &\times \left[\int_0^\infty dx f(x) \frac{\exp[-(x-\gamma\nu)^2/2(1-\gamma^2)]}{[2\pi(1-\gamma^2)]^{1/2}} \right] d\nu, \end{aligned} \quad (\text{B24})$$

where $x := -\nabla^2\delta/\sigma_2$ is the width of the peak and $f(x)$ is a function behaving $f(x) \rightarrow x^3 - 3x$ for large x . Note that x is also a statistical variable which is, in general, independent of ν .

For the perfect correlation of ν and x , $\gamma \rightarrow 1$, it reduces to

$$\mathcal{N}_{\text{pk}}(\nu) d\nu = \frac{1}{(2\pi)^2} \left(\frac{\sigma_2}{\sqrt{3}\sigma_1}\right)^3 e^{-\nu^2/2} f(\nu) d\nu. \quad (\text{B25})$$

In a finite volume V , the number of peaks that will collapse into PBHs, i.e., peaks of $\nu > \nu_{\text{th}}$, is given by

$$N_{\text{PBH}} = V \int_{\nu_{\text{th}}}^\infty \mathcal{N}_{\text{pk}}(\nu) d\nu. \quad (\text{B26})$$

The number of peaks in the range $(\nu, \nu + d\nu)$ in V is given by

$$n_{\text{PBH}}(\nu) d\nu = V \mathcal{N}_{\text{pk}}(\nu) d\nu. \quad (\text{B27})$$

Then, in the volume V , the probability distribution for one to find a peak in the range $(\nu, \nu + d\nu)$ from all the peaks greater than the threshold is given by

$$P_\nu(\nu) d\nu = \frac{n_{\text{PBH}}(\nu) d\nu}{N_{\text{PBH}}} = \frac{e^{-\nu^2/2} f(\nu) d\nu}{\int_{\nu_{\text{th}}}^\infty e^{-\bar{\nu}^2/2} f(\bar{\nu}) d\bar{\nu}}. \quad (\text{B28})$$

Therefore, the peak finding-condition is given by a Gaussian function with the correction factor $f(\nu)$. However, for peaks that will collapse into PBHs, the values of ν are always large such that $\nu > \nu_{\text{th}} \sim 10$. Thus, the Gaussian factor $e^{-\nu^2/2}$ rapidly decays for larger ν in the range $(\nu_{\text{th}}, \infty)$ and contributes to the probability distribution of PBH binaries, Eq. (28), only if $\nu \sim \nu_{\text{th}}$. Then, we can regard the factor $f(\nu) \sim f(\nu_{\text{th}})$ as a constant, which contributes to the overall factor. As a conclusion, we approximate the probability distribution as

$$P_\nu(\nu) d\nu = \frac{e^{-\nu^2/2} f(\nu) d\nu}{\int_{\nu_{\text{th}}}^\infty e^{-\bar{\nu}^2/2} f(\bar{\nu}) d\bar{\nu}} \simeq \frac{e^{-\nu^2/2} d\nu}{\int_{\nu_{\text{th}}}^\infty e^{-\bar{\nu}^2/2} d\bar{\nu}}, \quad (\text{B29})$$

as in Eq. (13).

As discussed in the end of Sec 3, the current PBH binary number has an uncertainty because, for example, we have applied numerical results obtained in works which assume spherical symmetry. We estimate the effect of this uncertainty in Appendix C and find that it somehow, but not greatly, changes the widths of the distribution. Thus, the above approximation, Eq. (B29), would not matter compared with this uncertainty.

C. MODIFICATION OF σ_0

As a modification of the peak threshold due to the uncertainty of the value of $\mathcal{C}_{\text{m,th}}$, we here show the numerical results of $P(\mathcal{M}, q, \chi_{\text{eff}})$ with different values of σ_0 . We take the values as $\sigma_0 = 0.128 (= (2/3) \times 0.192)$, 0.192 (the value taken in the main part), and 0.288 ($= (3/2) \times 0.192$). The results in Figs. 3–5 show that the distribution is somehow broadened (narrowed) for larger (smaller) σ_0 with fixed $\nu_{\text{th}} = 10$. In particular, the widths in χ_{eff} of $P(\chi_{\text{eff}}, q)$ are about 0.001, 0.0015, and 0.002 for $\sigma_0 = 0.288, 0.192$, and 0.128, respectively. Thus, we conclude that the uncertainty in the value of $\mathcal{C}_{\text{m,th}}$ does not greatly affect the distribution.

REFERENCES

Abbott, B. P., et al. 2018, Phys. Rev. Lett., 121, 161101, doi: [10.1103/PhysRevLett.121.161101](https://doi.org/10.1103/PhysRevLett.121.161101)

—. 2019, Phys. Rev. Lett., 123, 011102, doi: [10.1103/PhysRevLett.123.011102](https://doi.org/10.1103/PhysRevLett.123.011102)

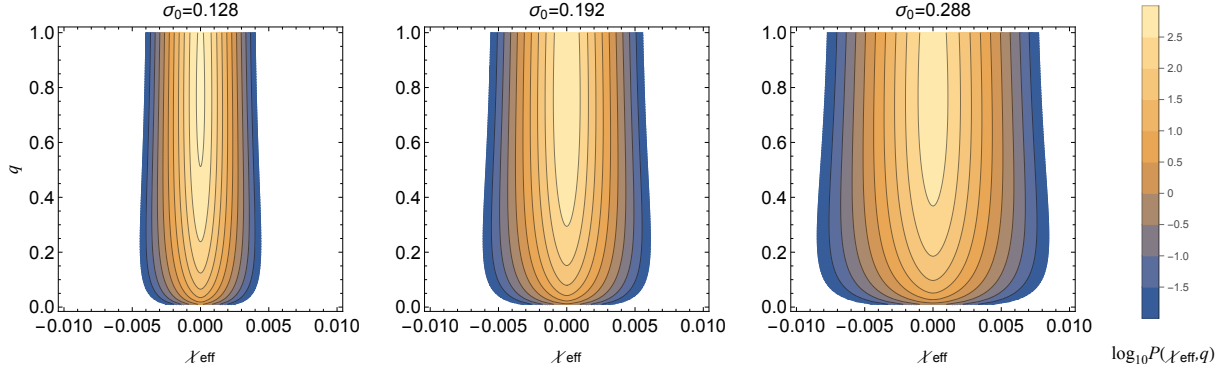


Figure 3. Contour plots of $\log_{10} P(\chi_{\text{eff}}, q)$ for $\sigma_0 = 0.128, 0.192,$ and 0.288 .

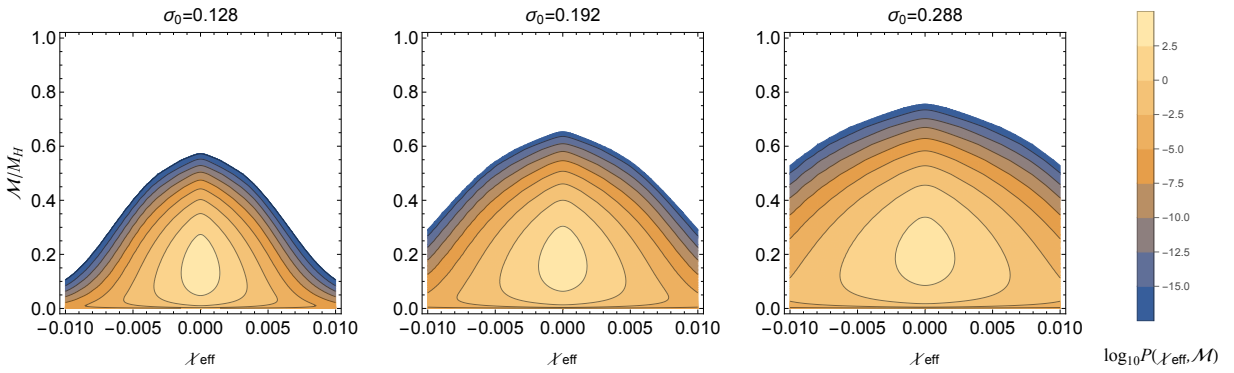


Figure 4. Contour plots of $\log_{10} P(\chi_{\text{eff}}, \mathcal{M})$ for $\sigma_0 = 0.128, 0.192,$ and 0.288 .

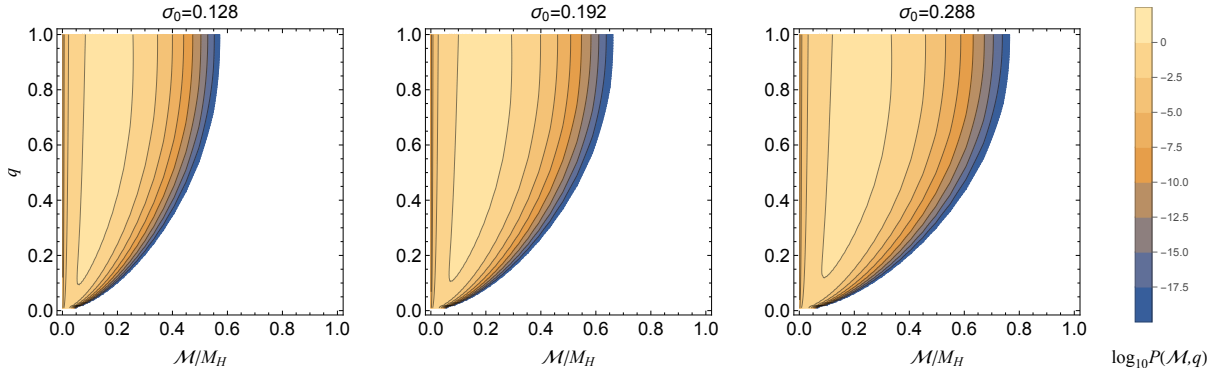


Figure 5. Contour plots of $\log_{10} P(\mathcal{M}, q)$ for $\sigma_0 = 0.128, 0.192,$ and 0.288 .

—. 2021a, *Astrophys. J.*, 909, 218,

doi: [10.3847/1538-4357/abdc67](https://doi.org/10.3847/1538-4357/abdc67)

Abbott, R., et al. 2020a, *Astrophys. J. Lett.*, 900, L13,

doi: [10.3847/2041-8213/aba493](https://doi.org/10.3847/2041-8213/aba493)

—. 2020b, *Astrophys. J. Lett.*, 896, L44,

doi: [10.3847/2041-8213/ab960f](https://doi.org/10.3847/2041-8213/ab960f)

—. 2021b. <https://arxiv.org/abs/2111.03606>

—. 2021c. <https://arxiv.org/abs/2112.06861>

—. 2021d. <https://arxiv.org/abs/2111.03634>

Aghanim, N., et al. 2020, *Astron. Astrophys.*, 641, A6,

doi: [10.1051/0004-6361/201833910](https://doi.org/10.1051/0004-6361/201833910)

Ali-Haïmoud, Y., Kovetz, E. D., & Kamionkowski, M. 2017,

Phys. Rev. D, 96, 123523,

doi: [10.1103/PhysRevD.96.123523](https://doi.org/10.1103/PhysRevD.96.123523)

Bardeen, J. M., Bond, J. R., Kaiser, N., & Szalay, A. S.

1986, *Astrophys. J.*, 304, 15, doi: [10.1086/164143](https://doi.org/10.1086/164143)

- Baumgarte, T. W., & Gundlach, C. 2016, *Phys. Rev. Lett.*, 116, 221103, doi: [10.1103/PhysRevLett.116.221103](https://doi.org/10.1103/PhysRevLett.116.221103)
- Bird, S., Cholis, I., Muñoz, J. B., et al. 2016, *Phys. Rev. Lett.*, 116, 201301, doi: [10.1103/PhysRevLett.116.201301](https://doi.org/10.1103/PhysRevLett.116.201301)
- Callister, T. A., Haster, C.-J., Ng, K. K. Y., Vitale, S., & Farr, W. M. 2021, *Astrophys. J. Lett.*, 922, L5, doi: [10.3847/2041-8213/ac2ccc](https://doi.org/10.3847/2041-8213/ac2ccc)
- Carr, B. J. 1975, *Astrophys. J.*, 201, 1, doi: [10.1086/153853](https://doi.org/10.1086/153853)
- . 2005. <https://arxiv.org/abs/astro-ph/0511743>
- Carr, B. J., & Hawking, S. W. 1974, *Mon. Not. Roy. Astron. Soc.*, 168, 399
- Celestino, J., & Baumgarte, T. W. 2018, *Phys. Rev. D*, 98, 024053, doi: [10.1103/PhysRevD.98.024053](https://doi.org/10.1103/PhysRevD.98.024053)
- Chiba, T., & Yokoyama, S. 2017, *PTEP*, 2017, 083E01, doi: [10.1093/ptep/ptx087](https://doi.org/10.1093/ptep/ptx087)
- Chongchitnan, S., & Silk, J. 2021, *Phys. Rev. D*, 104, 083018, doi: [10.1103/PhysRevD.104.083018](https://doi.org/10.1103/PhysRevD.104.083018)
- Clesse, S., & García-Bellido, J. 2017, *Phys. Dark Univ.*, 15, 142, doi: [10.1016/j.dark.2016.10.002](https://doi.org/10.1016/j.dark.2016.10.002)
- De Luca, V., Desjacques, V., Franciolini, G., Malhotra, A., & Riotto, A. 2019, *JCAP*, 05, 018, doi: [10.1088/1475-7516/2019/05/018](https://doi.org/10.1088/1475-7516/2019/05/018)
- De Luca, V., Franciolini, G., Pani, P., & Riotto, A. 2020, *JCAP*, 04, 052, doi: [10.1088/1475-7516/2020/04/052](https://doi.org/10.1088/1475-7516/2020/04/052)
- Eroshenko, Y. N. 2021, *JCAP*, 12, 041, doi: [10.1088/1475-7516/2021/12/041](https://doi.org/10.1088/1475-7516/2021/12/041)
- Escrivà, A. 2020, *Physics of the Dark Universe*, 27, 100466, doi: <https://doi.org/10.1016/j.dark.2020.100466>
- Escrivà, A., Germani, C., & Sheth, R. K. 2020, *Phys. Rev. D*, 101, 044022, doi: [10.1103/PhysRevD.101.044022](https://doi.org/10.1103/PhysRevD.101.044022)
- Evans, C. R., & Coleman, J. S. 1994, *Phys. Rev. Lett.*, 72, 1782, doi: [10.1103/PhysRevLett.72.1782](https://doi.org/10.1103/PhysRevLett.72.1782)
- Flores, M. M., & Kusenko, A. 2021, *Phys. Rev. D*, 104, 063008, doi: [10.1103/PhysRevD.104.063008](https://doi.org/10.1103/PhysRevD.104.063008)
- Germani, C., & Musco, I. 2019, *Phys. Rev. Lett.*, 122, 141302, doi: [10.1103/PhysRevLett.122.141302](https://doi.org/10.1103/PhysRevLett.122.141302)
- Green, A. M., & Liddle, A. R. 1999, *Phys. Rev. D*, 60, 063509, doi: [10.1103/PhysRevD.60.063509](https://doi.org/10.1103/PhysRevD.60.063509)
- Gundlach, C., & Baumgarte, T. W. 2016, *Phys. Rev. D*, 94, 084012, doi: [10.1103/PhysRevD.94.084012](https://doi.org/10.1103/PhysRevD.94.084012)
- Harada, T., Yoo, C.-M., & Kohri, K. 2013, *Phys. Rev. D*, 88, 084051, doi: [10.1103/PhysRevD.88.084051](https://doi.org/10.1103/PhysRevD.88.084051)
- Harada, T., Yoo, C.-M., Kohri, K., Koga, Y., & Monobe, T. 2021, *Astrophys. J.*, 908, 140, doi: [10.3847/1538-4357/abd9b9](https://doi.org/10.3847/1538-4357/abd9b9)
- Harada, T., Yoo, C.-M., Kohri, K., & Nakao, K.-I. 2017, *Phys. Rev. D*, 96, 083517, doi: [10.1103/PhysRevD.96.083517](https://doi.org/10.1103/PhysRevD.96.083517)
- Harada, T., Yoo, C.-M., Nakama, T., & Koga, Y. 2015, *Phys. Rev. D*, 91, 084057, doi: [10.1103/PhysRevD.91.084057](https://doi.org/10.1103/PhysRevD.91.084057)
- Hawking, S. 1971, *Mon. Not. Roy. Astron. Soc.*, 152, 75
- He, M., & Suyama, T. 2019, *Phys. Rev. D*, 100, 063520, doi: [10.1103/PhysRevD.100.063520](https://doi.org/10.1103/PhysRevD.100.063520)
- Heavens, A., & Peacock, J. 1988, *MNRAS*, 232, 339, doi: [10.1093/mnras/232.2.339](https://doi.org/10.1093/mnras/232.2.339)
- Koike, T., Hara, T., & Adachi, S. 1995, *Phys. Rev. Lett.*, 74, 5170, doi: [10.1103/PhysRevLett.74.5170](https://doi.org/10.1103/PhysRevLett.74.5170)
- Metzger, B. D. 2020, *Living Rev. Rel.*, 23, 1, doi: [10.1007/s41114-019-0024-0](https://doi.org/10.1007/s41114-019-0024-0)
- Mirbabayi, M., Gruzinov, A., & Noreña, J. 2020, *JCAP*, 03, 017, doi: [10.1088/1475-7516/2020/03/017](https://doi.org/10.1088/1475-7516/2020/03/017)
- Musco, I. 2019, *Phys. Rev. D*, 100, 123524, doi: [10.1103/PhysRevD.100.123524](https://doi.org/10.1103/PhysRevD.100.123524)
- Musco, I., & Miller, J. C. 2013, *Class. Quant. Grav.*, 30, 145009, doi: [10.1088/0264-9381/30/14/145009](https://doi.org/10.1088/0264-9381/30/14/145009)
- Musco, I., Miller, J. C., & Polnarev, A. G. 2009, *Class. Quant. Grav.*, 26, 235001, doi: [10.1088/0264-9381/26/23/235001](https://doi.org/10.1088/0264-9381/26/23/235001)
- Musco, I., Miller, J. C., & Rezzolla, L. 2005, *Class. Quant. Grav.*, 22, 1405, doi: [10.1088/0264-9381/22/7/013](https://doi.org/10.1088/0264-9381/22/7/013)
- Nadezhin, D., Novikov, I., & Polnarev, A. 1978, *Sov. Astron.*, 22, 129
- Nakamura, T., Sasaki, M., Tanaka, T., & Thorne, K. S. 1997, *Astrophys. J. Lett.*, 487, L139, doi: [10.1086/310886](https://doi.org/10.1086/310886)
- Niemeyer, J. C., & Jedamzik, K. 1998, *Phys. Rev. Lett.*, 80, 5481, doi: [10.1103/PhysRevLett.80.5481](https://doi.org/10.1103/PhysRevLett.80.5481)
- . 1999, *Phys. Rev. D*, 59, 124013, doi: [10.1103/PhysRevD.59.124013](https://doi.org/10.1103/PhysRevD.59.124013)
- Phukon, K. S., Baltus, G., Caudill, S., et al. 2021. <https://arxiv.org/abs/2105.11449>
- Sasaki, M., Suyama, T., Tanaka, T., & Yokoyama, S. 2016, *Phys. Rev. Lett.*, 117, 061101, doi: [10.1103/PhysRevLett.117.061101](https://doi.org/10.1103/PhysRevLett.117.061101)
- . 2018, *Class. Quant. Grav.*, 35, 063001, doi: [10.1088/1361-6382/aaa7b4](https://doi.org/10.1088/1361-6382/aaa7b4)
- Shibata, M., & Sasaki, M. 1999, *Phys. Rev. D*, 60, 084002, doi: [10.1103/PhysRevD.60.084002](https://doi.org/10.1103/PhysRevD.60.084002)
- Tada, Y., & Yokoyama, S. 2019, *Phys. Rev. D*, 100, 023537, doi: [10.1103/PhysRevD.100.023537](https://doi.org/10.1103/PhysRevD.100.023537)
- Vaskonen, V., & Veermäe, H. 2020, *Phys. Rev. D*, 101, 043015, doi: [10.1103/PhysRevD.101.043015](https://doi.org/10.1103/PhysRevD.101.043015)
- Yokoyama, J. 1998, *Phys. Rev. D*, 58, 107502, doi: [10.1103/PhysRevD.58.107502](https://doi.org/10.1103/PhysRevD.58.107502)
- Yoo, C.-M., Harada, T., Garriga, J., & Kohri, K. 2018, *Prog. Theor. Exp. Phys.*, 2018, 123E01. <https://arxiv.org/abs/1805.03946>

Zel'dovich, Y. B., & Novikov, I. D. 1967, *Soviet Astron. AJ*
(Engl. Transl.), 10, 602